

Mu-Tau Reflection Symmetry in the Standard Parametrization and Contributions from Charged Lepton Sector

Chandan Duarah ¹

Department of Physics, Dibrugarh University, Dibrugarh - 786004, India

Abstract

The $\mu - \tau$ reflection symmetry of the lepton mixing matrix accommodates maximal atmospheric mixing ($\theta_{23} = \pi/4$) as well as maximal Dirac CP phase ($\delta = \pm\pi/2$) for the Dirac case. In the standard parametrization of the PMNS matrix the reflection symmetric nature is not directly visible while substituting the maximal values of the mixing parameters. This issue has been addressed in this paper. It is found that the reflection symmetry in the 'standard' PMNS matrix can be restored by allowing maximal values of the Majorana CP phases (α, β) as well, along with maximal δ . To accommodate non-maximal values of θ_{23} and δ we consider charged lepton contributions to the neutrino mixing and implement the proposed scheme of reflection symmetry in the neutrino mixing matrix. The charged lepton correction scheme succeeds in the prediction of lepton mixing parameters consistent with the global 3ν oscillation data.

Key-words: Lepton mixing, $\mu - \tau$ reflection symmetry, charged lepton contributions.

PACS number: 14.60 Pq

arXiv:2006.01639v2 [hep-ph] 1 Apr 2021

¹E-mail: chandan.duarah@gmail.com

1 Introduction

The measurement of the non-zero reactor angle θ_{13} [1–3] elevates neutrino physics research one step ahead. It also initiates the exploration of leptonic CP violation in oscillation experiments. The Dirac CP violating phase δ is likely to be determined soon with good accuracy whereas the problems of octant degeneracy and mass ordering still require their solutions. Recent data from T2K [4], NO ν A [5] and IceCube [6] experiments indicates a preference for the atmospheric angle θ_{23} to lie in the second octant which is also reflected in the global analysis of neutrino oscillation data made in Refs. [7,8]. The global analysis also indicates that the value of δ is close to $-\pi/2$.

The approximate mixing pattern revealed by the oscillation data stems the main motivation towards $\mu - \tau$ flavour symmetry to understand the theory of lepton mixing. The near maximal value of the atmospheric mixing angle θ_{23} predicted by oscillation data is the key point behind $\mu - \tau$ flavour symmetry. The flavour symmetry, mostly exercised in lepton flavour models, is the so called $\mu - \tau$ permutation symmetry. It accommodates the well known predictions- $\theta_{23} = \pi/4$ and $\theta_{13} = 0$, that dominates the field of neutrino physics research over a long period of time. The permutation symmetry embedded with a CP conjugation of the lepton sector is referred to as the $\mu - \tau$ reflection symmetry. This concept of $\mu - \tau$ reflection symmetry was first put forwarded by Harrison and Scott [9]. Subsequently the mass matrix bearing the reflection symmetry property is realized in a A_4 based model by Babu, Ma and Valle [10] and a general treatment of the reflection symmetry is rendered in Ref. [11]. A review of $\mu - \tau$ flavour symmetry is also available in Ref. [12].

The prediction $\theta_{23} = \pi/4$ is a common feature of $\mu - \tau$ symmetry and of course θ_{12} remains arbitrary in either cases. However the two types of symmetry differ by their predictions on θ_{13} and the CP phase δ . In case of $\mu - \tau$ permutation symmetry δ is washed out in the standard parametrization of PMNS matrix, as a consequence of $\theta_{13} = 0$. Thereby $\mu - \tau$ permutation symmetry naturally corresponds to CP conservation. In contrast to $\mu - \tau$ permutation symmetry, the reflection symmetry is featured with a non-zero θ_{13} and in addition, it corresponds to a maximal value of the CP phase ($\delta = \pm\pi/2$). We can also note down that in the standard parametrization, if we restrict θ_{13} to be zero, $\mu - \tau$ reflection symmetry readily reproduces the properties of permutation symmetry. In that sense $\mu - \tau$ reflection symmetry is a more general symmetry that can accommodate non-zero θ_{13} as well as CP violation.

Bi-maximal (BM) mixing and tri-bimaximal (TBM) mixing are two special cases of $\mu - \tau$ permutation symmetry. It is obvious that these special mixing schemes or in general the permutation symmetric models are mostly explored in the phenomenological studies of lepton mixing. In the present scenario, after the discovery of non zero θ_{13} , permutation symmetry is seemingly an inadequate theory as it can not accommodate non-zero θ_{13} and the CP violation. In this regard $\mu - \tau$ reflection symmetry might serve a precious role in neutrino physics research. In comparison to the permutation symmetry, $\mu - \tau$ reflection symmetry and its possible phenomenological implications are less studied. The predictions $\theta_{23} = \pi/4$ and $\delta = \pm\pi/2$ are the central point of any $\mu - \tau$ reflection symmetric model. Such models incorporated with non abelian discrete symmetries and their significance have been discussed in Refs. [13–18]. The implementation of reflection symmetry in see-saw mechanism and the scenario of broken symmetry under renormalization group running effects are studied in Refs. [19–22]. Phenomenological consequences in other scenarios can be found in Refs. [23–27].

Though $\mu - \tau$ reflection symmetry corresponds to the predictions- $\theta_{23} = \pi/4$ and $\delta = \pm\pi/2$, we can notice that the reflection symmetric nature of the mixing matrix can not be viewed by direct

substitution of these values in the lepton mixing matrix in standard parametrization. This is in contrast to $\mu - \tau$ permutation symmetry where its predictions ($\theta_{23} = \pi/4$ and $\theta_{13} = 0$) directly results into a $\mu - \tau$ (permutation) symmetric mixing matrix upon substitution. We have addressed this issue in this work and seek possible solutions to restore the symmetry in the standard parametrization. A full parametrization of the lepton mixing matrix with three mixing angles and six phases is considered and specific choice of the phases is found to serve the purpose of this work. Besides the maximal Dirac phase δ , as accommodated by reflection symmetry itself, we are led to additionally set maximal values of Majorana phases (α and β) too in order to restore reflection symmetry property of the lepton mixing matrix.

In view of the oscillation data, a small deviation of θ_{23} from its maximal value is also notable. A perturbation which can break the symmetry is necessary to account for the desired deviations. We consider the contributions from charged lepton sector as a possible scheme to deviate θ_{23} and δ from their maximal values. In a basis where charged lepton mass matrix is non-diagonal, the charged lepton mixing matrix is allowed to break the reflection symmetry of the neutrino mixing matrix. The charged lepton mixing matrix can be parametrized in terms three mixing angles and three complex phases. All of them act as free parameters in the present study. On the neutrino sector atmospheric angle and the Dirac phase assume maximal values through reflection symmetry while other two mixing angles remain unconstrained. The lepton mixing angles basically depend on the corresponding neutrino mixing angles with small contributions from the charged lepton mixing parameters. It is the purpose of this work to study in what way the various free parameters influence the predictions of the lepton mixing angles. The correlation between the free parameters and the lepton mixing angles are studied and possible values of the free parameters are examined on the basis of numerical analysis.

The paper is organised as follow: in section 2 we outline the basic ingredients of lepton mixing which are necessary for the present study. In section 3 we briefly review $\mu - \tau$ reflection symmetry and discuss the ambiguity addressed. Section 4 discusses the scenario of broken reflection symmetry under the charged lepton correction scheme. Finally in section 5 we summarize and conclude the work.

2 Ingredients of lepton mixing

Standard model charged current interaction Lagrangian for the leptons in flavour basis is given by

$$\mathcal{L}_{int} = -\frac{g}{\sqrt{2}}\bar{l}'_L\gamma^\mu\nu'_L W_\mu^- + h.c., \quad (1)$$

where $l'_L = (e' \ \mu' \ \tau')^T_L$ and $\nu'_L = (\nu'_e \ \nu'_\mu \ \nu'_\tau)^T_L$ represent the left handed charged lepton flavour states and neutrino flavour states respectively. In transforming to mass basis we get the lepton mixing U , also known as the PMNS matrix, in the Lagrangian :

$$\mathcal{L}_{int} = -\frac{g}{\sqrt{2}}\bar{l}_L\gamma^\mu U\nu_L W_\mu^- + h.c.. \quad (2)$$

The un-primed fields, viz. $l_L = (e \ \mu \ \tau)^T_L$ and $\nu_L = (\nu_1 \ \nu_2 \ \nu_3)^T_L$, denote the respective mass eigenstates. We define the diagonalizing matrices U_l and U_ν for the charged lepton and Majorana

Mixing Parameter	Best fit	3 σ
$\sin^2 \theta_{12}$	0.310	0.275 - 0.350
$\sin^2 \theta_{23}$	0.580	0.418 - 0.627
$\sin^2 \theta_{13}$	0.0224	0.0204 - 0.0244
δ	215°	125° - 392°

Table 1: Best fit and 3σ values of mixing parameters for normal hierarchy (NH) from global analysis [8].

neutrino mass matrices respectively as : $U_l^\dagger M_l^\dagger M_l U_l = M_{ld}^2 \equiv \text{Diag}(m_e^2, m_\mu^2, m_\tau^2)$ and $U_\nu^\dagger M_\nu U_\nu^* = M_{\nu d} \equiv \text{Diag}(m_1, m_2, m_3)$, such that the PMNS matrix is given by

$$U = U_l^\dagger U_\nu. \quad (3)$$

If we choose the basis where flavour eigenstates and mass eigenstates of the charged leptons are identical, the charged lepton mixing matrix U_l in Eq.(3) becomes an identity matrix. The PMNS matrix U , which is a unitary matrix, can be parametrized in terms three mixing angles and six phases. In a familiar parametrization U can be expressed as

$$U = P_1 V P_2, \quad (4)$$

where the mixing matrix V is parametrized in terms of the three mixing angles ($\theta_{12}, \theta_{12}, \theta_{12}$) and the Dirac CP phase δ . The diagonal phase matrix $P_2 = \text{diag}(e^{i\alpha}, e^{i\beta}, 1)$ contains two Majorana phases α and β while $P_1 = \text{diag}(e^{i\phi_1}, e^{i\phi_2}, e^{i\phi_3})$ contains the remaining three phases. The three phases in P_1 are un-physical which can be eliminated from the mixing matrix U by phase redefinition of the charged lepton fields. In the standard parametrization we have

$$V = \begin{pmatrix} c_{12}c_{13} & s_{12}c_{13} & s_{13}e^{-i\delta} \\ -s_{12}c_{23} - c_{12}s_{23}s_{13}e^{i\delta} & c_{12}c_{23} - s_{12}s_{23}s_{13}e^{i\delta} & s_{23}c_{13} \\ s_{12}s_{23} - c_{12}c_{23}s_{13}e^{i\delta} & -c_{12}s_{23} - s_{12}c_{23}s_{13}e^{i\delta} & c_{23}c_{13} \end{pmatrix}, \quad (5)$$

where $s_{ij} = \sin \theta_{ij}$ and $c_{ij} = \cos \theta_{ij}$ with $ij = 12, 23, 13$. So far physical observables are concerned, one may simply drop P_1 from Eq.(4). If neutrinos are considered as Dirac particles P_2 can further be dropped in a particular study.

Turning to the mixing angles, the sine of the angles can be expressed in terms of the absolute values of the elements of U as follows :

$$\sin^2 \theta_{13} = |U_{e3}|^2, \quad \sin^2 \theta_{12} = \frac{|U_{e2}|^2}{1 - |U_{e3}|^2}, \quad \sin^2 \theta_{23} = \frac{|U_{\mu 3}|^2}{1 - |U_{e3}|^2}. \quad (6)$$

The measure of CP violation is expressed in terms of parametrization independent quantities called rephasing invariants. We consider the Jarlskog invariant [28] given by

$$J = \text{Im}[U_{e2}U_{\mu 3}U_{e3}^*U_{\mu 2}^*], \quad (7)$$

for our analysis. For the mixing matrix V in Eq.(5), Eq.(7) yields

$$J = s_{12}c_{12}s_{23}c_{23}s_{13}c_{13}^2 \sin \delta. \quad (8)$$

The best fit and 3σ values of the three mixing angles and the Dirac CP phase for normal hierarchy (NH) are presented in Table 1 from the global analysis [8].

3 $\mu - \tau$ reflection symmetry

To begin with, we first consider the flavor basis where charged lepton mass matrix is diagonal such that there is no contribution to the PMNS matrix U in Eq.(3) from the charged lepton mixing matrix U_l . The discussion made in this section will be concerned with the PMNS matrix without any charged lepton correction. In the next section we will turn into the flavor basis with a non diagonal charged lepton mass matrix and its effects on the PMNS matrix will be studied.

The original formulation of $\mu - \tau$ reflection symmetry, introduced by Harrison and Scott [9], concerns the Dirac phase δ only where Majorana phases are dropped from the lepton mixing matrix. In the present consideration it is represented by the mixing matrix V in Eq.(5). They were motivated from the observation that the modulus of each μ -flavor element of the mixing matrix is approximately equal to that of the corresponding τ -flavor element (i.e. $|V_{\mu i}| \simeq |V_{\tau i}|$), as revealed by the neutrino oscillation data. They follow a specific parametrization of the mixing matrix based on the assumption $|U_{\mu i}| = |U_{\tau i}|$, and arrive at the mixing matrix

$$V_{HS} = \begin{pmatrix} u_1 & u_2 & u_3 \\ v_1 & v_2 & v_3 \\ v_1^* & v_2^* & v_3^* \end{pmatrix}, \quad (9)$$

where u_i 's are taken as real and v_i 's as complex. This mixing matrix is symmetric under a combined operation of interchanging ν_μ and ν_τ flavour states and complex conjugation of the mixing matrix. This combined operation of symmetry is referred to as $\mu - \tau$ reflection symmetry. The corresponding mass matrix is required to invariant under the $\mu - \tau$ reflection operation which can be expressed as

$$(A_{\mu\tau} M A_{\mu\tau})^* = M, \quad (10)$$

where

$$A_{\mu\tau} = \begin{pmatrix} 1 & 0 & 0 \\ 0 & 0 & 1 \\ 0 & 1 & 0 \end{pmatrix}, \quad (11)$$

is the $\mu - \tau$ exchange operator. The mass matrix satisfying Eq.(10) is given by

$$M = \begin{pmatrix} M_{ee} & M_{e\mu} & M_{e\mu}^* \\ M_{e\mu} & M_{\mu\mu} & M_{\mu\tau} \\ M_{e\mu}^* & M_{\mu\tau} & M_{\mu\mu}^* \end{pmatrix}, \quad (12)$$

where the elements M_{ee} and $M_{\mu\tau}$ are real. This mass matrix were reproduced in an A_4 based model by Babu, Ma and Valle, one year after the concept of reflection symmetry introduced. The crucial thing about the mixing matrix V_{HS} is that it is linked with the aforementioned predictions- $\theta_{23} = \pi/4$ and $\delta = \pm\pi/2$. To see this connection let us consider the Jarlskog's invariant for V_{HS} which is given by $J = \frac{1}{2}u_1u_2u_3$, as obtained from Ref. [9]. In terms of mixing matrix elements modulus of J can be written as

$$|J| = \frac{1}{2}|V_{e1}V_{e2}V_{e3}|. \quad (13)$$

Again in the standard parametrization, from Eq.(8) we have

$$|J| = \frac{1}{2}|V_{e1}V_{e2}V_{e3}||\sin \delta| \sin 2\theta_{23}. \quad (14)$$

For non zero θ_{13} , comparison of Eqs.(13) and (14) gives $|\sin \delta| \sin 2\theta_{23} = 1$. For $\theta_{23} = \pi/4$, this implies $\delta = \pm\pi/2$.

Conversely we may now wish to see whether the mixing matrix V in Eq.(5), with $\theta_{23} = \pi/4$ and $\delta = \pm\pi/2$, reflect the reflection symmetric nature of V_{HS} or not. To be explicit, we have

$$V = \begin{pmatrix} c_{12}c_{13} & s_{12}c_{13} & \mp i s_{13} \\ \frac{1}{\sqrt{2}}(-s_{12} \mp i c_{12}s_{13}) & \frac{1}{\sqrt{2}}(c_{12} \mp i s_{12}s_{13}) & \frac{c_{13}}{\sqrt{2}} \\ \frac{1}{\sqrt{2}}(s_{12} \mp i c_{12}s_{13}) & \frac{1}{\sqrt{2}}(-c_{12} \mp i s_{12}s_{13}) & \frac{c_{13}}{\sqrt{2}} \end{pmatrix}, \quad (15)$$

from Eq.(5), where 'mp' sign corresponds to $\delta = \pm\pi/2$. We can see that the matrix reproduces the presumed conditions : $|U_{\mu i}| = |U_{\tau i}|$, as expected. However μ and τ -flavour mixing elements of V do not satisfy $V_{\tau j} = V_{\mu j}^*$ (followed from Eq.(9)), instead we have $V_{\tau j} = -V_{\mu j}^*$ for $j = 1, 2$ while $V_{\tau 3} = V_{\mu 3}^*$. Further, most significantly, first row elements of the mixing matrix are not real which necessarily violates the inherent reflection symmetric nature carried by V_{HS} . That means the PMNS matrix in the standard parametrization does not exhibit reflection symmetry under the constraints $\theta_{23} = \pi/4$ and $\delta = \pm\pi/2$. It is however necessary to point out that the mass matrix diagonalized by V in Eq.(15) respects reflection symmetry (Eq.(12)).

To realize the properties of reflection symmetry in the 'standard' PMNS matrix consistent with $\theta_{23} = \pi/4$ and $\delta = \pm\pi/2$, we find it useful to consider the full parametrization defined in Eq.(4). All the six phases taken into account, we get the PMNS matrix from Eq.(4) as

$$U = \begin{pmatrix} V_{e1}e^{i(\alpha+\phi_1)} & V_{e2}e^{i(\beta+\phi_1)} & V_{e3}e^{i\phi_1} \\ V_{\mu 1}e^{i(\alpha+\phi_2)} & V_{\mu 2}e^{i(\beta+\phi_2)} & V_{\mu 3}e^{i\phi_2} \\ V_{\tau 1}e^{i(\alpha+\phi_3)} & V_{\tau 2}e^{i(\beta+\phi_3)} & V_{\tau 3}e^{i\phi_3} \end{pmatrix}, \quad (16)$$

with the elements V_{lj} ($l = e, \mu, \tau; j = 1, 2, 3$) defined through Eq.(5). Compared to the 'Dirac like' mixing matrix V (Eq.(5)), concerned with the original formulation of reflection symmetry, we now have five additional phases under consideration. With $\theta_{23} = \pi/4$ and $\delta = \pm\pi/2$ the elements V_{lj} are given in Eq.(15). We find that the reflection symmetric nature of V_{HS} can be restored in U with proper choice of these additional phases. Let us first consider the case $\delta = \pi/2$. We then conveniently choose $\phi_1 = \pi/2$ and $\alpha = \beta = -(\pi/2)$ to make the first row elements all real. In addition the remaining two phases are constrained to zero ($\phi_2 = \phi_3 = 0$). With these specific values of the phases the PMNS matrix in Eq.(16) becomes

$$U = \begin{pmatrix} c_{12}c_{13} & s_{12}c_{13} & s_{13} \\ \frac{1}{\sqrt{2}}s(-c_{12}s_{13}) + i s_{12} & \frac{1}{\sqrt{2}}(-s_{12}s_{13} - i c_{12}) & \frac{c_{13}}{\sqrt{2}} \\ \frac{1}{\sqrt{2}}(-c_{12}s_{13}) - i s_{12} & \frac{1}{\sqrt{2}}(-s_{12}s_{13} + i c_{12}) & \frac{c_{13}}{\sqrt{2}} \end{pmatrix}. \quad (17)$$

This matrix is now exactly similar to V_{HS} with the first row elements all real and second and third row elements satisfying the condition $U_{\tau j} = U_{\mu j}^*$ for all $j = 1, 2, 3$. The specific values of the un-physical phases so chosen may be attributed to the arbitrariness in their values. Besides, the values of the Majorana phases are remarkable. It is meant that, in addition to maximal δ , Majorana phases are also enforced to pick up maximal values in order to restore the symmetry. For the other case with $\delta = -\pi/2$, we may have the choices: $\phi_1 = -\pi/2$ and $\alpha = \beta = (\pi/2)$, which differ by a negative sign in comparison to the previous set of values. The other two phases ϕ_2 and

ϕ_3 should be kept fixed at zero as before. The resulting PMNS matrix, containing the reflection symmetry, is similar to that in Eq.(17) but with the elements $U_{\mu 1}$ and $U_{\mu 2}$ replaced by complex conjugation of the respective elements of U in Eq.(17). In other sense the two mixing matrices are related by

$$U_{\delta=-\pi/2} = U_{\delta=\pi/2}^* \quad (18)$$

where $U_{\delta=\pi/2}$ represents the matrix in Eq.(17).

In the basis where charged lepton mass matrix is already diagonal, the Majorana neutrino mass matrix can be obtained from $M = U M_{\nu d} U^T$. The mixing matrix in Eq.(17) leads to a mass matrix satisfying the reflection symmetry as shown by M in Eq.(12). The elements are given by

$$\begin{aligned} M_{ee} &= (m_1 c_{12}^2 + m_2 s_{12}^2) c_{13}^2 + m_3 s_{13}^2, \\ M_{\mu\tau} &= \frac{1}{2} m_1 (c_{12}^2 s_{13}^2 + s_{12}^2) + \frac{1}{2} m_2 (s_{12}^2 s_{13}^2 + c_{12}^2) + \frac{1}{2} m_3 c_{13}^2, \\ M_{e\mu} &= \frac{1}{\sqrt{2}} (-m_1 c_{12}^2 - m_2 s_{12}^2 + m_3) s_{13} c_{13} + \frac{i}{\sqrt{2}} (m_1 - m_2) s_{12} c_{12} c_{13}, \\ M_{\mu\mu} &= \frac{1}{2} \left[m_1 (c_{12}^2 s_{13}^2 - s_{12}^2) + m_2 (s_{12}^2 s_{13}^2 - c_{12}^2) + m_3 c_{13}^2 \right] - i(m_1 - m_2) s_{12} c_{12} s_{13}. \end{aligned} \quad (19)$$

For the case $\theta_{23} = \pi/4$ and $\delta = -\pi/2$, the mass matrix obtained from $U_{\delta=-\pi/2}$ follows a similar connection as presented in Eq.(18). The mass matrices of the two cases are complex conjugate of each other ($M_{\delta=-\pi/2} = M_{\delta=\pi/2}^*$).

4 Charged lepton contributions

If the values of θ_{23} and δ are not exactly maximal, one has to deviate from the reflection symmetry in some way. Possible corrections from the charged lepton sector are often considered in this regard [29–40]. To employ the charged lepton correction scheme we recall Eq.(3) and define the lepton mixing matrix as

$$\tilde{U}^{MNS} = (\tilde{U}^l)^\dagger U^\nu, \quad (20)$$

in the basis where charged lepton mass matrix is non-diagonal. Under this basis the lepton mixing matrix will contain contributions from both \tilde{U}^l and U^ν . The common idea of this approach is to assume a perfect symmetry in either of the two sectors (\tilde{U}^l or U^ν) and then perturb this symmetry by the other leading to a desired lepton mixing matrix. A treatment involving both the alternate cases is available in Ref. [29]. The symmetry considered in most works is the $\mu - \tau$ permutation symmetry which incorporates maximal atmospheric angle and zero reactor angle while solar angle is left arbitrary. Since Bimaximal mixing and Tri-bimaximal mixing are two special cases of $\mu - \tau$ permutation symmetry, deviations from such special mixing through charged lepton correction is most common. However corrections to special mixing based on $\mu - \tau$ reflection symmetry from charged lepton sector is very rare in the literature.

Each of \tilde{U}^l and U^ν is a unitary matrix and can be parametrized in terms of three mixing angles and six phases as well. We invoke the parametrization set up presented in Eq.(4) to define both the mixing matrices and we get

$$\tilde{U}^l = P_1^l V^l P_2^l, \quad U^\nu = P_1^\nu V^\nu P_2^\nu. \quad (21)$$

With the above matrices the resulting PMNS matrix in Eq.(20) becomes

$$\tilde{U}^{MNS} = (P_2^l)^\dagger (V^l)^\dagger (P_1^l)^\dagger P_1^\nu V^\nu P_2^\nu. \quad (22)$$

The diagonal phase matrices are defined as : $P_1^l = \text{diag}(e^{i\phi_1^l}, e^{i\phi_2^l}, e^{i\phi_3^l})$, $P_2^l = \text{diag}(e^{i\alpha^l}, e^{i\beta^l}, 1)$, $P_1^\nu = \text{diag}(e^{i\phi_1^\nu}, e^{i\phi_2^\nu}, e^{i\phi_3^\nu})$, $P_2^\nu = \text{diag}(e^{i\alpha^\nu}, e^{i\beta^\nu}, 1)$; while the matrices V^l and V^ν resemble V in Eq.(5), given by

$$V^l = \begin{pmatrix} c_{12}^l c_{13}^l & s_{12}^l c_{13}^l & s_{13}^l e^{-i\delta^l} \\ -s_{12}^l c_{23}^l - c_{12}^l s_{23}^l s_{13}^l e^{i\delta^l} & c_{12}^l c_{23}^l - s_{12}^l s_{23}^l s_{13}^l e^{i\delta^l} & s_{23}^l c_{13}^l \\ s_{12}^l s_{23}^l - c_{12}^l c_{23}^l s_{13}^l e^{i\delta^l} & -c_{12}^l s_{23}^l - s_{12}^l c_{23}^l s_{13}^l e^{i\delta^l} & c_{23}^l c_{13}^l \end{pmatrix}, \quad (23)$$

$$V^\nu = \begin{pmatrix} c_{12}^\nu c_{13}^\nu & s_{12}^\nu c_{13}^\nu & s_{13}^\nu e^{-i\delta^\nu} \\ -s_{12}^\nu c_{23}^\nu - c_{12}^\nu s_{23}^\nu s_{13}^\nu e^{i\delta^\nu} & c_{12}^\nu c_{23}^\nu - s_{12}^\nu s_{23}^\nu s_{13}^\nu e^{i\delta^\nu} & s_{23}^\nu c_{13}^\nu \\ s_{12}^\nu s_{23}^\nu - c_{12}^\nu c_{23}^\nu s_{13}^\nu e^{i\delta^\nu} & -c_{12}^\nu s_{23}^\nu - s_{12}^\nu c_{23}^\nu s_{13}^\nu e^{i\delta^\nu} & c_{23}^\nu c_{13}^\nu \end{pmatrix}. \quad (24)$$

To take into account charged lepton contributions we now assume the exact $\mu - \tau$ reflection symmetry, presented in section 3, in the neutrino sector and let this symmetry perturb by the the charged lepton mixing matrix \tilde{U}^l . We set the specific values of the neutrino mixing parameters as : $\theta_{23}^\nu = \pi/4$, $\delta^\nu = \pm\pi/2$, $\alpha^\nu = \beta^\nu = \mp\pi/2$, $\phi_1^\nu = \pm\pi/2$ and $\phi_2^\nu = \phi_3^\nu = 0$. With these substitutions we get the reflection symmetric neutrino mixing matrix given by

$$U^\nu = \begin{pmatrix} c_{12}^\nu c_{13}^\nu & s_{12}^\nu c_{13}^\nu & s_{13}^\nu \\ \frac{1}{\sqrt{2}} (-c_{12}^\nu s_{13}^\nu \pm i s_{12}^\nu) & \frac{1}{\sqrt{2}} (-s_{12}^\nu s_{13}^\nu \mp i c_{12}^\nu) & \frac{1}{\sqrt{2}} c_{13}^\nu \\ \frac{1}{\sqrt{2}} (-c_{12}^\nu s_{13}^\nu \mp i s_{12}^\nu) & \frac{1}{\sqrt{2}} (-s_{12}^\nu s_{13}^\nu \pm i c_{12}^\nu) & \frac{1}{\sqrt{2}} c_{13}^\nu \end{pmatrix}, \quad (25)$$

in Eq.(22). The '±' signs in the '21'-element of the above mixing matrix correspond to the two different cases- viz., *Case I*: $\theta_{23}^\nu = \pi/4$, $\delta^\nu = +\pi/2$; and *Case II*: $\theta_{23}^\nu = \pi/4$, $\delta^\nu = -\pi/2$; respectively.

The mixing angles θ_{12}^ν and θ_{13}^ν in U^ν in Eq.(25) are left arbitrary by the reflection symmetry. After having this reflection symmetric neutrino mixing matrix, we are left with the charged lepton mixing matrix \tilde{U}^l in Eq.(22). All the mixing parameters in \tilde{U}^l , viz., three mixing angles- θ_{12}^l , θ_{23}^l , θ_{13}^l , and six phases- δ^l , α^l , β^l , ϕ_1^l , ϕ_2^l , ϕ_3^l , remain as free parameters in the model. In total we have eleven free parameters that determine the mixing parameters of the PMNS matrix \tilde{U}^{MNS} in Eq.(22). However we can identify three of the six phases in \tilde{U}^l as un-physical and the total number of free parameters can be reduced. Note that \tilde{U}^{MNS} is also parametrized in the same manner as \tilde{U}^l and U^ν which is given by

$$\tilde{U}^{MNS} = P_1^{MNS} V^{MNS} P_2^{MNS}, \quad (26)$$

with $P_1^{MNS} = \text{diag}(e^{i\phi_1}, e^{i\phi_2}, e^{i\phi_3})$, $P_2^{MNS} = \text{diag}(e^{i\alpha}, e^{i\beta}, 1)$ and V^{MNS} given by Eq.(5). This PMNS matrix contains total six phases out of which the three phases in the phase matrix P_1^{MNS} are un-physical. Again from Eq.(22) we see that five out of the six phases of \tilde{U}^l are distributed in the phase matrices P_1^l and P_2^l . We can commute P_1^l to the left of the right hand side of Eq.(22) and it helps us to identify the un-physical phases present in Eq.(22). By doing so, Eq.(22) can be re-expressed as

$$\tilde{U}^{MNS} = (P^l)^\dagger (U^l)^\dagger U^\nu, \quad (27)$$

where $(P^l)^\dagger = (P_2^l)^\dagger(P_1^l)^\dagger$ and $(U^l)^\dagger$ is given by

$$\begin{pmatrix} c_{12}^l c_{13}^l & s_{12}^l c_{23}^l e^{i\delta_{12}^l} - c_{12}^l s_{23}^l s_{13}^l e^{-i(\delta_{23}^l - \delta_{13}^l)} & s_{12}^l s_{23}^l e^{i(\delta_{12}^l + \delta_{23}^l)} - c_{12}^l c_{23}^l s_{13}^l e^{i\delta_{13}^l} \\ s_{12}^l c_{13}^l e^{-i\delta_{12}^l} & c_{12}^l c_{23}^l - s_{12}^l s_{23}^l s_{13}^l e^{-i(\delta_{12}^l + \delta_{23}^l - \delta_{13}^l)} & -c_{12}^l s_{23}^l e^{i\delta_{23}^l} - s_{12}^l c_{23}^l s_{13}^l e^{-i(\delta_{12}^l - \delta_{13}^l)} \\ s_{13}^l e^{-i\delta_{13}^l} & s_{23}^l c_{13}^l e^{-i\delta_{23}^l} & c_{23}^l c_{13}^l \end{pmatrix}. \quad (28)$$

Above charged lepton mixing matrix is derived from the relation $(U^l)^\dagger = (U_{12}^l)^\dagger(U_{13}^l)^\dagger(U_{23}^l)^\dagger$, where the form of the rotation matrices U_{12}^l , U_{13}^l and U_{23}^l are presented in appendix A with each mixing parameter symbolized with the superscript l . The phases newly defined in U^l satisfy the relations

$$\delta_{12}^l = \phi_1^l - \phi_2^l, \quad \delta_{13}^l = \delta^l - \phi_1^l + \phi_3^l, \quad \delta_{23}^l = \phi_2^l - \phi_3^l. \quad (29)$$

In view of Eqs.(26) and (27), we can now drop the phase matrices P_1^{MNS} and $(P^l)^\dagger$ from these equations as they stand for the un-physical phases. The resulting PMNS matrix is given by

$$V^{MNS} P_2^{MNS} = U^{MNS} = (U^l)^\dagger U^\nu, \quad (30)$$

with U^l and U^ν given in Eqs.(28) and (25) respectively. The PMNS matrix in Eq.(30), now contains the Dirac phase δ and the Majorana phases α and β only on the left hand side. After the elimination of the un-physical phases, number of free parameters on the right hand side of Eq.(30) reduces to eight with three complex phases from the charged lepton sector. The mixing angles and the CP phases of U^{MNS} will be the functions of these eight free parameters.

Naturally it is expected that the lepton mixing angles θ_{12} , θ_{23} and θ_{13} receive their major contributions from the respective neutrino mixing angles $(\theta_{12}^\nu, \theta_{23}^\nu, \theta_{13}^\nu)$ with small contributions from the charged lepton sector. By the recent discovery third angle θ_{13} is found to be very small compared to the other two. By the same token we can expect θ_{13}^ν ($\sim \theta_{13}$), to be very small compared to θ_{12}^ν and θ_{23}^ν . To analyze the consequences of Eq.(30) we are interested to consider a mixing matrix U^l with small mixing angles θ_{12}^l , θ_{23}^l and θ_{13}^l [29,32]. Under this consideration it is useful to define the parameters $\sin \theta_{ij}^l = \lambda_{ij} > 0$ with $ij = 12, 23, 13$. As θ_{13}^ν should be smaller than θ_{13} , we can assume an upper bound ~ 0.15 for $\sin \theta_{13}^\nu$ as per the best fit value of $\sin \theta_{13}$ [8]. Under such situation we also have $O(s_{13}^\nu) \sim O(\lambda_{ij})$ for the small λ_{ij} 's. With these parameters mixing matrix U^l in Eq.(28) becomes

$$(U^l)^\dagger \approx \begin{pmatrix} 1 - \frac{1}{2}\lambda_{12}^2 - \frac{1}{2}\lambda_{13}^2 & -\lambda_{12}e^{i\delta_{12}^l} - \lambda_{23}\lambda_{13}e^{-i(\delta_{23}^l - \delta_{13}^l)} & -\lambda_{13}e^{i\delta_{13}^l} - \lambda_{12}\lambda_{23}e^{i(\delta_{12}^l + \delta_{23}^l)} \\ \lambda_{12}e^{-i\delta_{12}^l} & 1 - \frac{1}{2}\lambda_{12}^2 - \frac{1}{2}\lambda_{23}^2 & -\lambda_{23}e^{i\delta_{23}^l} - \lambda_{12}\lambda_{13}e^{-i(\delta_{12}^l - \delta_{13}^l)} \\ \lambda_{13}e^{-i\delta_{13}^l} & \lambda_{23}e^{-i\delta_{23}^l} & 1 - \frac{1}{2}\lambda_{23}^2 - \frac{1}{2}\lambda_{13}^2 \end{pmatrix}, \quad (31)$$

where higher order terms with λ_{ij}^n ($n > 2$) are neglected for the small angles. The elements of U^{MNS} are then given by Eqs.(30), (31) and (25). For convenience we write down the following three elements:

$$\begin{aligned} U_{e3}^{MNS} &\simeq \sin \theta_{13}^\nu - \frac{1}{\sqrt{2}} \left(\lambda_{12}e^{i\delta_{12}^l} + \lambda_{13}e^{i\delta_{13}^l} \right) \\ &\quad + \frac{1}{\sqrt{2}} \left(\lambda_{12}\lambda_{23}e^{i(\delta_{12}^l + \delta_{23}^l)} - \lambda_{23}\lambda_{13}e^{-i(\delta_{23}^l - \delta_{13}^l)} \right), \end{aligned} \quad (32)$$

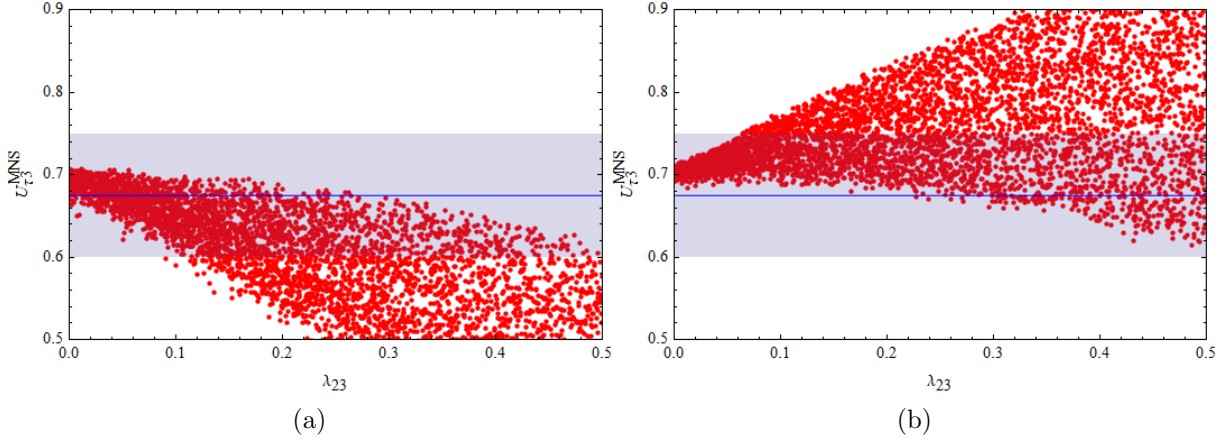


Figure 1: Correlation between $U_{\tau 3}^{MNS}$ and λ_{23} for (a) negative values of $\cos \delta_{23}^l$ and (b) positive values of $\cos \delta_{23}^l$. Horizontal coloured bands represent the 3σ range and the blue lines stand for the best fit value of $U_{\tau 3}^{MNS}$ obtained from global data.

$$U_{\mu 3}^{MNS} \simeq \frac{1}{\sqrt{2}} - \frac{1}{\sqrt{2}} \lambda_{23} e^{i\delta_{23}^l} + \sin \theta_{13}^\nu \lambda_{12} e^{-i\delta_{12}^l} - \frac{1}{2\sqrt{2}} \left(\lambda_{12}^2 + \lambda_{23}^2 + \sin^2 \theta_{13}^\nu + 2\lambda_{12}\lambda_{13} e^{-i(\delta_{12}^l - \delta_{13}^l)} \right), \quad (33)$$

$$U_{\tau 3}^{MNS} \simeq \frac{1}{\sqrt{2}} + \frac{1}{\sqrt{2}} \lambda_{23} e^{-i\delta_{23}^l} + \sin \theta_{13}^\nu \lambda_{13} e^{-i\delta_{13}^l} - \frac{1}{2\sqrt{2}} \left(\lambda_{23}^2 + \lambda_{13}^2 + \sin^2 \theta_{13}^\nu \right), \quad (34)$$

It can be noted from the left side of Eq.(30) that ' $\mu 3$ ' and ' $\tau 3$ ' elements of the PMNS matrix are free from the Majorana CP phases and are also real. Comparing the real and imaginary parts of Eq.(34) we get

$$\cos \theta_{23} \cos \theta_{13} = \frac{1}{\sqrt{2}} + \frac{1}{\sqrt{2}} \lambda_{23} \cos \delta_{23}^l + s_{13}^\nu \lambda_{13} \cos \delta_{13}^l - \frac{1}{2\sqrt{2}} \left(\lambda_{23}^2 + \lambda_{13}^2 + (s_{13}^\nu)^2 \right), \quad (35)$$

$$\sin \theta_{13}^\nu = -\frac{1}{\sqrt{2}} \frac{\lambda_{23} \sin \delta_{23}^l}{\lambda_{13} \sin \delta_{13}^l}, \quad (36)$$

and the imaginary parts of Eq.(33) give

$$\sin \theta_{13}^\nu = -\frac{1}{\sqrt{2}} \frac{\lambda_{23} \sin \delta_{23}^l - \lambda_{12} \lambda_{13} \sin(\delta_{12}^l - \delta_{13}^l)}{\lambda_{12} \sin \delta_{12}^l}. \quad (37)$$

Expressions (36) and (37) show the interconnection between the free parameters of U^l and $\sin \theta_{13}^\nu$. These two equations can be used to constrain any two of the free parameters. The factor $1/\sqrt{2}$ in Eq.(35) carries the sign of maximal atmospheric mixing while the second term contributes as first order in λ_{ij} . Rest of the terms in this expression account for the second order contributions which are relatively very small. We first study the correlation between $U_{\tau 3}^{MNS}$ and λ_{23} from Eq.(35) with $0 < s_{13}^\nu \leq 0.15$ and an approximate bound of $0-0.25$ for λ_{13} . We find that $\cos \delta_{23}^l$ plays a significant role in predicting $U_{\tau 3}^{MNS}$ within the observed bound of global data. We inspect the correlation

separately for positive values ($0 \leq \cos \delta_{23}^l \leq 1$) as well as negative values ($-1 \leq \cos \delta_{23}^l \leq 0$) for δ_{23}^l and relevant plots are depicted in Fig.1. From these plots it is clear that negative values of $\cos \delta_{23}^l$, corresponding to $(\pi/2) \leq \delta_{23}^l \leq (3\pi/2)$, are preferable to accommodate best fit value of $U_{\tau 3}^{MNS}$. In rest of the analyzes we will consider this range for δ_{23}^l . Again for negative $\cos \delta_{23}^l$, sine of δ_{23}^l can be positive ($(\pi/2) \leq \delta_{23}^l < \pi$) as well as negative ($\pi < \delta_{23}^l \leq (3\pi/2)$). From Eq.(36) it can be seen that, as both λ_{23} and λ_{13} are positive, the relative sign between $\sin \delta_{23}^l$ and $\sin \delta_{13}^l$ should be negative in order to have $\sin \theta_{13}^\nu > 0$.

From Eq.(32) we get

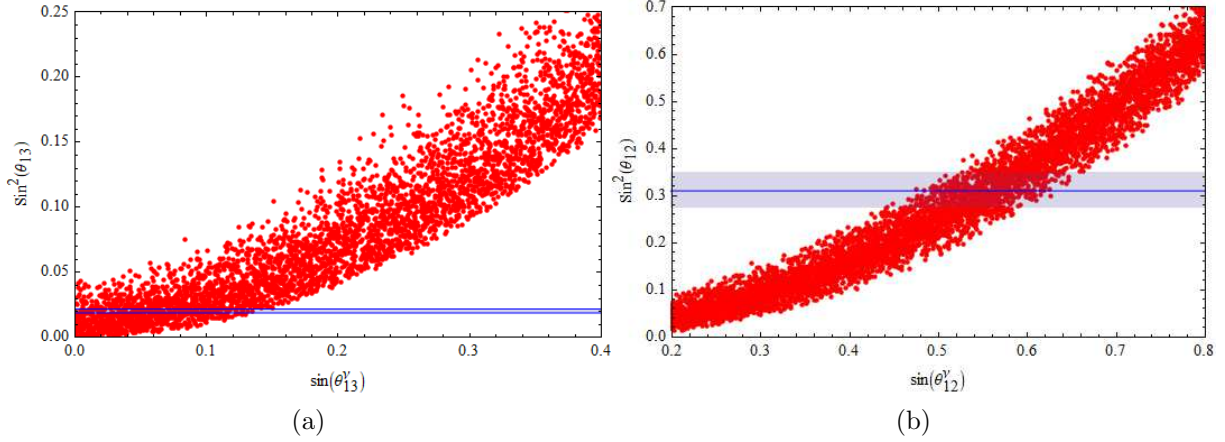


Figure 2: (a) Correlation between $\sin^2 \theta_{13}$ and $\sin \theta_{13}^\nu$. Horizontal blue band represents the 3σ range of $\sin^2 \theta_{13}$. (b) Correlation between $\sin^2 \theta_{12}$ and $\sin \theta_{12}^\nu$. Horizontal colored band and the blue line represent the 3σ range and the best fit value of $\sin^2 \theta_{12}$ respectively.

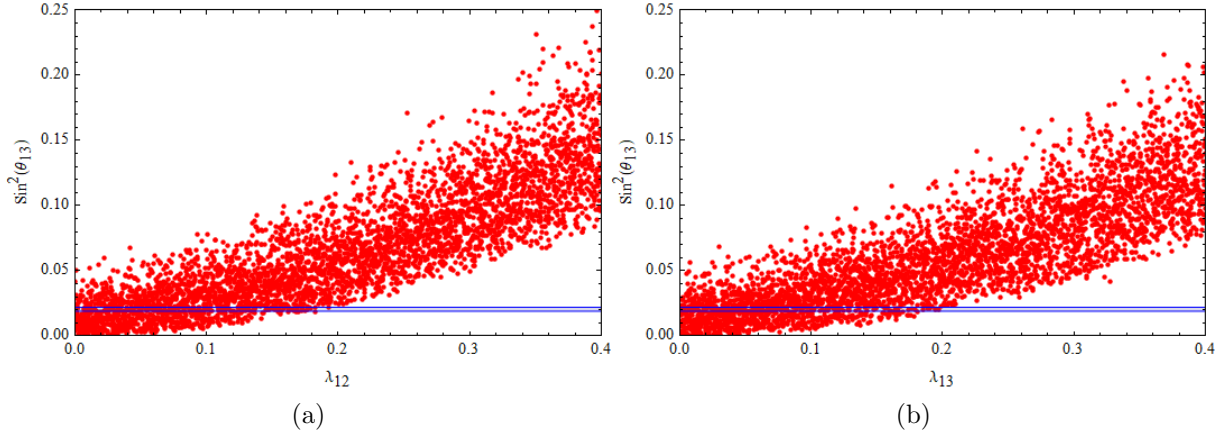


Figure 3: (a) Correlation between $\sin^2 \theta_{13}$ and λ_{12} and (b) that of $\sin^2 \theta_{13}$ and λ_{13} . Horizontal blue bands represent the 3σ range of $\sin^2 \theta_{13}$.

$$\begin{aligned}\sin^2 \theta_{13} &\simeq \sin^2 \theta_{13}^\nu - \sqrt{2} \sin \theta_{13}^\nu \left(\lambda_{12} \cos \delta_{12}^l + \lambda_{13} \cos \delta_{13}^l \right) \\ &\quad + \frac{1}{2} \left(\lambda_{12}^2 + \lambda_{13}^2 + 2\lambda_{12}\lambda_{13} \cos(\delta_{12}^l - \delta_{13}^l) \right).\end{aligned}\quad (38)$$

The sine of other two mixing angles can be obtained using Eq.(6) and are given by

$$\begin{aligned}\sin^2 \theta_{23} &\simeq \frac{1}{2} - \lambda_{23} \cos \delta_{23}^l + \frac{1}{\sqrt{2}} \sin \theta_{13}^\nu \left(\lambda_{12} \cos \delta_{12}^l - \lambda_{13} \cos \delta_{13}^l \right) \\ &\quad - \frac{1}{4} \left(\lambda_{12}^2 - \lambda_{13}^2 \right) - \frac{1}{2} \lambda_{12} \lambda_{13} \cos(\delta_{12}^l - \delta_{13}^l),\end{aligned}\quad (39)$$

$$\begin{aligned}\sin^2 \theta_{12} &\simeq \sin^2 \theta_{12}^\nu \mp \frac{1}{\sqrt{2}} \sin 2\theta_{12}^\nu \left(\lambda_{12} \sin \delta_{12}^l - \lambda_{13} \sin \delta_{13}^l \right) \\ &\quad + \left(\frac{1}{2} - \sin^2 \theta_{12}^\nu \right) \left[\lambda_{12}^2 + \lambda_{13}^2 - 2\lambda_{12}\lambda_{13} \cos(\delta_{12}^l - \delta_{13}^l) \right] \\ &\quad \mp \frac{1}{\sqrt{2}} \sin 2\theta_{12}^\nu \left[\lambda_{12}\lambda_{23} \sin(\delta_{12}^l + \delta_{23}^l) - \lambda_{23}\lambda_{13} \sin(\delta_{23}^l - \delta_{13}^l) \right].\end{aligned}\quad (40)$$

In the above expressions we have considered the terms up to second order in λ_{ij} . The ' \mp ' signs in the second term of right hand side of Eq.(40) correspond to Case I and Case II respectively. The correlation between $\sin^2 \theta_{13}$ and $\sin \theta_{13}^\nu$ is shown in Fig. 2(a) where the best fit value of $\sin \theta_{13} = 0.149$ (Table 1). From this plot we can see that the allowed values of $\sin \theta_{13}^\nu$ are less than $\sin \theta_{13}$ as expected. The correlation between $\sin^2 \theta_{12}$ and $\sin \theta_{12}^\nu$ (Fig. 2(b)) shows a positive linear relationship. An allowed range of 0.5 – 0.6 can be read off the correlation plot for $\sin \theta_{12}^\nu$ corresponding to the best fit value of $\sin^2 \theta_{12}$ (0.556). We have also studied the correlation between $\sin^2 \theta_{13}$ and λ_{12} and λ_{13} and are presented in Fig. 3(a) and 3(b) respectively. These plots reflect that the values of the free parameters λ_{12} and λ_{13} may be taken closed to 0.1. Similar observation can also be made for λ_{23} from Fig. 1(a). In these correlation studies negative values of both $\cos \delta_{12}^l$ and $\cos \delta_{13}^l$ are found to be preferable along with negative $\cos \delta_{23}^l$.

From the real and imaginary parts of Eq.(32) we can express the Dirac CP phase δ of the lepton mixing matrix in terms of the free parameters. It is given by

$$\tan \delta = \frac{\lambda_{12} \sin \delta_{12} + \lambda_{13} \sin \delta_{13} - \lambda_{12}\lambda_{23} \sin(\delta_{12}^l + \delta_{23}^l) - \lambda_{23}\lambda_{13} \sin(\delta_{23}^l - \delta_{13}^l)}{\sqrt{2}s_{13}^\nu - \lambda_{12} \cos \delta_{12} - \lambda_{13} \cos \delta_{13} + \lambda_{12}\lambda_{23} \cos(\delta_{12}^l + \delta_{23}^l) - \lambda_{23}\lambda_{13} \cos(\delta_{23}^l - \delta_{13}^l)}.\quad (41)$$

The Jarlskog invariant can be obtained using Eq.(7) and is found to be

$$\begin{aligned}J &\simeq \pm \frac{1}{2} s_{12}^\nu c_{12}^\nu s_{13}^\nu (c_{13}^\nu)^2 \mp \frac{1}{2\sqrt{2}} s_{12}^\nu c_{12}^\nu (c_{13}^\nu)^3 \left(\lambda_{12} \cos \delta_{12}^l + \lambda_{13} \cos \delta_{13}^l \right) \\ &\quad + \frac{1}{2\sqrt{2}} \left[(s_{12}^\nu)^2 (c_{13}^\nu)^2 - (c_{12}^\nu)^2 \right] s_{13}^\nu c_{13}^\nu \left(\lambda_{12} \sin \delta_{12}^l - \lambda_{13} \sin \delta_{13}^l \right) \\ &\quad \pm \frac{1}{2\sqrt{2}} s_{12}^\nu c_{12}^\nu (c_{13}^\nu)^3 \left[\lambda_{12}\lambda_{23} \cos(\delta_{12}^l - \delta_{23}^l) - \lambda_{23}\lambda_{13} \cos(\delta_{23}^l + \delta_{13}^l) \right] \\ &\quad - \frac{1}{2} \left[(s_{12}^\nu)^2 (c_{13}^\nu)^2 - (c_{12}^\nu)^2 \right] (c_{13}^\nu)^2 \lambda_{12}\lambda_{13} \sin(\delta_{12}^l - \delta_{13}^l),\end{aligned}\quad (42)$$

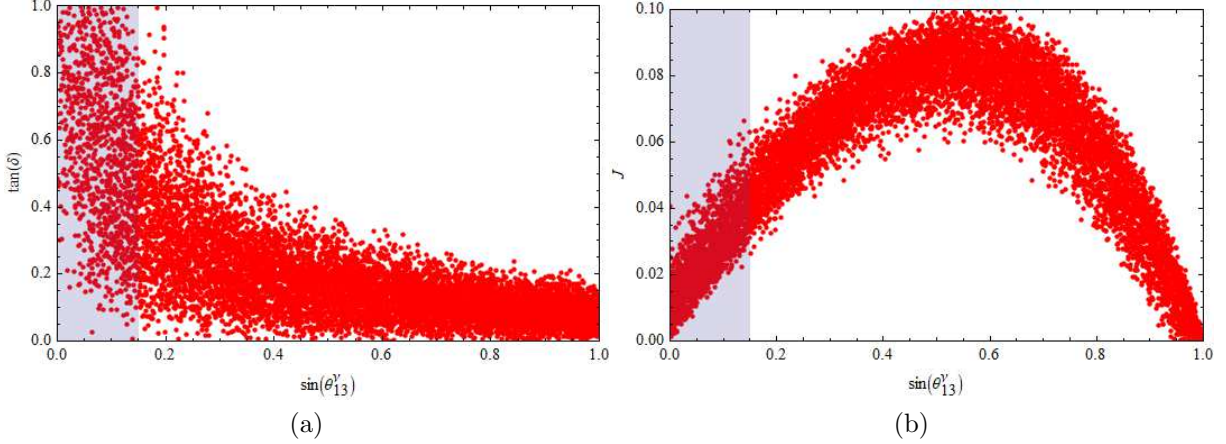


Figure 4: (a) Correlation between $\tan \delta$ and $\sin \theta'_{13}$ and (b) that of J and $\sin \theta'_{13}$. Vertical blue bands represent the allowed range of $\sin \theta'_{13}$.

where ' \pm ' signs in the first term of right hand side correspond to Case I and Case II respectively.

Fig. 4(a) shows the correlation between $\tan \delta$ and $\sin \theta'_{13}$. As per the global best fit value $\tan \delta = 0.7$ (Table 1), we see that the predictions of $\tan \delta$ are consistent with the observed data within the allowed range of $\sin \theta'_{13}$ (0 – 0.15). The correlation between J and $\sin \theta'_{13}$ (Fig 4(b)) is also consistent with the global analysis data [8] which estimates a maximal possible value of 0.033 for the Jarlskog invariant.

A numerical analysis considering different possible input values for the eight free parameters is in order. To perform the analysis we first choose the values of the two mixing angles θ'_{13} and θ'_{12} of the neutrino mixing matrix U^ν . We analyze two different cases with $\sin \theta'_{13} = 0.05$ and 0.1. For both the cases neutrino solar angle is taken to be $\sin \theta'_{12} = 0.55$. To choose the values of the free parameters of U^l we start with Eq.(36). As reflected from the correlation studies, we are interested in the values of λ_{ij} 's that are lying near to 0.1. We run the analysis considering three types of values for λ_{23} and λ_{13} : $\lambda_{23} < \lambda_{13}$, $\lambda_{23} > \lambda_{13}$ and $\lambda_{23} = \lambda_{13}$. Specifically we have considered the values- 0.05/0.1, 0.1/0.05 and 0.1/0.1 for $\lambda_{23}/\lambda_{13}$ for a given value of $\sin \theta'_{13}$. After having the values of $\sin \theta'_{13}$, λ_{23} and λ_{13} fixed, Eq.(36) allows us to choose some possible values of $\sin \delta'_{23}$ and $\sin \delta'_{13}$. It is seen that with the chosen values of $\sin \theta'_{13}$, λ_{23} and λ_{13} , Eq.(36) constrains the values of $\sin \delta'_{23}$ and $\sin \delta'_{13}$ to a very narrow range. Remaining two free parameters (λ_{12} and δ'_{12}) can finally be chosen using Eq.(37). For a given set of values of $\sin \theta'_{13}$ and λ_{23} , λ_{13} , δ'_{23} and δ'_{13} , we vary the values of λ_{12} in steps of 0.05 and the corresponding values of $\sin \delta'_{12}$ are solved from Eq.(37).

It is important to note that ' $e3$ ', ' $\mu3$ ' and ' $\tau3$ ' elements of U^{MNS} remain unaltered for the two cases : Case I and Case II, and thereby predictions of $\sin^2 \theta_{13}$ (Eq.(38)), $\sin^2 \theta_{23}$ (Eq.(39)) and $\tan \delta$ (Eq.(41)) remain same for both the cases. However, other elements of U^{MNS} become different for the two cases due to the effect of ' \pm ' signs and consequently the expressions for $\sin^2 \theta_{12}$ (Eq.(40)) and J (Eq.(42)) suffer changes. Let us first consider Case I ($\theta'_{23} = \pi/4$, $\delta^\nu = +\pi/2$). The different input values of the parameters of charged lepton mixing matrix U^l with $\sin \theta'_{13} = 0.05$ and $\sin \theta'_{12} = 0.55$ and corresponding predictions of the lepton mixing angles are presented in Table 2. Similar numerical predictions with same type of input values of the parameters of U^l are

$\sin \theta_{13}^\nu = 0.05; \sin \theta_{12}^\nu = 0.55$										
λ_{12}	λ_{23}	λ_{13}	$\delta_{12}^l/^\circ$	$\delta_{23}^l/^\circ$	$\delta_{13}^l/^\circ$	$\sin^2 \theta_{12}$	$\sin^2 \theta_{23}$	$\sin^2 \theta_{13}$	$\tan \delta$	J
$\lambda_{23} < \lambda_{13}$										
0.05	0.05	0.1	245	174	225	0.282	0.550	0.019	0.717	0.0252
0.1	0.05	0.1	225	174	225	0.298	0.545	0.032	0.663	0.0328
0.15	0.05	0.1	218	174	225	0.313	0.538	0.047	0.633	0.0395
$\lambda_{23} > \lambda_{13}$										
0.05	0.1	0.05	196	179	196	0.300	0.598	0.014	0.170	0.0260
0.1	0.1	0.05	191	179	196	0.304	0.594	0.025	0.158	0.0342
0.15	0.1	0.05	190	179	196	0.309	0.589	0.038	0.150	0.0421
$\lambda_{23} = \lambda_{13}$										
0.05	0.1	0.1	246	177	226	0.278	0.601	0.018	0.730	0.0242
0.1	0.1	0.1	225	177	226	0.293	0.595	0.032	0.671	0.0321
0.15	0.1	0.1	219	177	226	0.306	0.589	0.048	0.640	0.0390

Table 2: Input values of the free parameters of U^l and U^ν and corresponding predictions of the PMNS matrix parameters.

$\sin \theta_{13}^\nu = 0.1; \sin \theta_{12}^\nu = 0.55$										
λ_{12}	λ_{23}	λ_{13}	$\delta_{12}^l/^\circ$	$\delta_{23}^l/^\circ$	$\delta_{13}^l/^\circ$	$\sin^2 \theta_{12}$	$\sin^2 \theta_{23}$	$\sin^2 \theta_{13}$	$\tan \delta$	J
$\lambda_{23} > \lambda_{13}$										
0.05	0.1	0.05	227	177	227	0.297	0.598	0.024	0.349	0.0322
0.1	0.1	0.05	208	177	227	0.305	0.592	0.039	0.318	0.0405
0.15	0.1	0.05	203	177	227	0.313	0.586	0.056	0.300	0.0479
$\lambda_{23} = \lambda_{13}$										
0.05	0.1	0.1	244	175	218	0.285	0.603	0.033	0.440	0.0359
0.1	0.1	0.1	218	175	218	0.294	0.595	0.051	0.406	0.0444
0.15	0.1	0.1	210	175	218	0.303	0.587	0.071	0.386	0.0514

Table 3: Input values of the free parameters of U^l and U^ν and corresponding predictions of the PMNS matrix parameters.

$\sin \theta_{13}^\nu = 0.05; \sin \theta_{12}^\nu = 0.55$										
λ_{12}	λ_{23}	λ_{13}	$\delta_{12}^l/^\circ$	$\delta_{23}^l/^\circ$	$\delta_{13}^l/^\circ$	$\sin^2 \theta_{12}$	$\sin^2 \theta_{23}$	$\sin^2 \theta_{13}$	$\tan \delta$	J
0.05	0.05	0.1	245	174	225	0.324	0.550	0.019	0.717	-0.0250
0.05	0.1	0.05	196	179	196	0.304	0.598	0.014	0.170	-0.0261
0.05	0.1	0.1	246	177	226	0.328	0.601	0.018	0.730	-0.0241

Table 4: Input values of the free parameters of U^l and U^ν and corresponding predictions of the PMNS matrix parameters.

presented in Table 3 for $\sin \theta'_{13} = 0.1$ and $\sin \theta'_{12} = 0.55$. Few significant remarks can be drawn from this numerical analysis regarding the connection between λ_{ij} 's and the lepton mixing angles. The value of the atmospheric mixing angle θ_{23} mainly depends on λ_{23} while the effects of the other two parameters ($\lambda_{12}, \lambda_{13}$) are relatively small. It can also be observed from Eq.(39) where the first factor $1/2$ stands for the maximal value of $\sin^2 \theta_{23}$. The value of λ_{23} together with $\cos \delta'_{23}$ accounts for the deviation of θ_{23} from the maximal value without any significant effect from λ_{12} and λ_{13} . Further, since λ_{23} is positive, the sign of $\cos \delta'_{23}$ basically determines the octant for θ_{23} . As per the indication $\sin^2 \theta_{23} > 0.5$, revealed by oscillation data, we constrain $\cos \delta'_{23}$ to negative values in the present analysis. Eq.(38) shows that the prediction on reactor angle θ_{13} depends both on λ_{12} and λ_{13} and corresponding phases in the leading order while the effect of λ_{23} is negligible. The same is also visible in the numerical results. The first block of Table 2 displays the predictions of the lepton mixing angles for the fixed value of $\lambda_{23} = 0.05$ while those of second and third blocks correspond to $\lambda_{23} = 0.1$. The predictions of $\sin^2 \theta_{23}$ corresponding to $\lambda_{23} = 0.05$ are less than the global best fit value (0.58) while those corresponding to $\lambda_{23} = 0.1$ are obtained at the desired level. We can see that while varying λ_{12} for a fixed ($\lambda_{23}/\lambda_{13}$), $\sin^2 \theta_{23}$ does not change significantly. This suggests that value of λ_{23} closed to 0.1 is suitable to generate the observed atmospheric mixing angle in the second octant. The prediction of $\sin^2 \theta_{13}$ depends both on λ_{12} or λ_{13} . From Tables 2 and 3 we can see that for a fixed value of λ_{23} , $\sin^2 \theta_{13}$ gradually increases either with λ_{12} or λ_{13} . As per the global best fit value of $\sin^2 \theta_{13} = 0.022$, we observe that the values of $\lambda_{12} \sim 0.05$ (or 0.1) and $\lambda_{13} \sim 0.1$ (or 0.05) may serve the desired purpose. However, as the orders of $\sin \theta'_{13}$ and λ_{ij} 's are same, relative magnitudes of $\sin \theta'_{13}$, λ_{12} and λ_{13} play certain role in the prediction of $\sin^2 \theta_{13}$. A comparative analysis on the prediction of $\sin^2 \theta_{13}$ can be made from Table 2 and Table 3. We find that the predictions of $\sin^2 \theta_{13}$ are relatively higher for $\sin \theta'_{13} = 0.1$ compared to $\sin \theta'_{13} = 0.05$. Hence the choices $\sin \theta'_{13} < 0.1$ are preferable in predicting the third lepton mixing angle θ_{13} at its global best fit value for input values of $\lambda_{12}, \lambda_{13} \sim 0.1$. The prediction on solar angle θ_{12} basically depends on θ'_{12} with small perturbation from the small λ_{ij} 's. We first analyze the predictions taking input values for $\sin \theta'_{12} < 0.55$ where 0.55 is the global best fit value of $\sin \theta_{12}$. As the predictions of $\sin^2 \theta_{12}$ are found to be less than that of the global best fit (0.31), we compute the analysis assuming $\sin \theta'_{12} \approx \sin \theta_{12} = 0.55$. Corresponding results can be read from Table 2 and Table 3.

Turning to the prediction of the Dirac CP violation effects, we note that the global analysis of 3ν oscillation data [8] provides a best fit value of $\tan \delta = 0.7$ for normal hierarchy (Table 1). Further, it indicates a value of the Jarlskog invariant $J = -0.019$ for non-maximal mixing. In view of these predictions we can compare the results of Table 2 and Table 3 and we find that the choice $\sin \theta'_{13} = 0.05$ is more suitable. It is also reflected from the correlation plot of J and $\sin \theta'_{13}$ (Fig. 4(b)) that lower values of $\sin \theta'_{13}$ correspond to smaller values of J . Regarding the prediction of $\tan \delta$, we however notice a difference in the second block of Table 2 where the predicted values are significantly small as compared to the global best fit.

In view of the overall prediction of the lepton mixing parameters we can find particular interest in the results of Table 2 obtained for $\sin \theta'_{13} = 0.05$ and $\sin \theta'_{12} = 0.55$. We can see that the input values $(\lambda_{12}, \lambda_{23}, \lambda_{13}) = (0.1, 0.1, 0.05)$ (second block) can generate the three mixing angles at the desired best fit values. However the prediction on $\tan \delta$ is not consistent with the global best fit value. Moving to the third block, the input values $(\lambda_{12}, \lambda_{23}, \lambda_{13}) = (0.05, 0.1, 0.1)$ are also good in predicting all the parameters at desired level except for the solar angle which lies below the global best fit value. Although the prediction of $\sin^2 \theta_{12}$ can be lifted by increasing the

value of λ_{12} , it, in turn, affects the prediction of $\sin^2 \theta_{13}$. It is interesting to note that the best fit value of $\sin^2 \theta_{12}$ can be maintained without affecting the prediction of $\sin^2 \theta_{13}$ in the other case (Case II). Numerical predictions with different input values for Case II are presented in Table 4. We can compare the predictions of the mixing parameters in the two cases for the input values $(\lambda_{12}, \lambda_{23}, \lambda_{13}) = (0.05, 0.1, 0.1)$ from Table 2 and Table 4 which shows that prediction on $\sin^2 \theta_{12}$ rises from 0.278 to 0.328.

5 Summary and conclusion

The role of $\mu - \tau$ reflection symmetry, as it features a non zero θ_{13} besides maximal θ_{23} , is significant in the study of lepton flavour models. In this work we point out that the reflection symmetric nature of the lepton mixing matrix is not reflected back while substituting the maximal values of θ_{23} and δ in the standard parametrization. Motivated by this observation we look for possible solution to this ambiguity and find that the symmetry can be restored by assigning maximal values of the Majorana phases as well in addition to maximal Dirac phase δ . A noteworthy contribution from the un-physical phases is remarked in the symmetry realization.

We have exercised the scenario under a broken symmetry such that deviated values of maximal θ_{23} and maximal δ can be accommodated. For this purpose, contributions from charged lepton sector is considered as a possible scheme to generate the broken symmetry. We implant the reflection symmetry in the neutrino mixing matrix U^ν and study the consequences in the lepton mixing matrix under the basis where the charged lepton mass matrix is non diagonal. The perturbations from the charged lepton sector are assumed to be small and the mixing matrix U^l is parametrized in terms of the small parameters λ_{ij} 's ($ij = 12, 23, 13$). The parametrization of U^l , in addition, includes three complex phases δ_{12}^l , δ_{23}^l and δ_{13}^l . The predictions of the lepton mixing parameters of U^{MNS} depend on the six free parameters of U^l along with θ_{13}^ν and θ_{12}^ν of U^ν . A comprehensive numerical analysis is made in this work regarding the possible values of the free parameters in determining desired lepton mixing parameters. We primarily focus on the possible values of the parameters λ_{ij} 's and the two neutrino mixing angles. The values of λ_{ij} 's are found to be in the order of 0.1 to generate the lepton mixing parameters consistent with global data. It is apparent that the lepton mixing angles are close to the values of the corresponding neutrino mixing angles with small perturbations from λ_{ij} 's. Reflection symmetry fixes the neutrino atmospheric angle at the maximal value $\sin^2 \theta_{23}^\nu = 1/2$. As per the global best fit value of $\sin^2 \theta_{23} = 0.58$, we expect a slight positive contribution from the charged lepton mixing parameters. In the charged lepton correction scheme considered, λ_{23} along with the associating phase δ_{23}^l is found to play the chief role in this regard. Values of $\lambda_{23} \lesssim 0.1$ and negative values of $\cos \delta_{23}^l$ are suitable to generate the global best fit value of $\sin^2 \theta_{23}$. For the neutrino solar angle, values of $\sin \theta_{12}^\nu \lesssim \sin \theta_{12}$ are found to provide the desired predictions. There exists a distinction between the predictions of $\sin^2 \theta_{12}$ in the two separate cases (Case I and Case II). Prediction of $\sin^2 \theta_{12}$ is better with respect to the global best fit value in Case II ($\theta_{23}^\nu = \pi/4$, $\delta^\nu = -\pi/2$). Prediction of $\sin^2 \theta_{13}$ depends on both $\sin \theta_{13}^\nu$ and the parameters λ_{12} and λ_{13} under the same order. It is observed that values of $\sin \theta_{13}^\nu \ll 0.15$ (global best fit value of $\sin \theta_{13}$) are more comfortable corresponding to the input values of $\lambda_{12}, \lambda_{13} \sim 0.1$. Such small values of $\sin \theta_{13}^\nu$ are also preferable in predicting small non maximal values of the Jarlskog invariant as indicated by global analysis data. The Dirac CP violation effect is observed in terms of $\tan \delta$. It's prediction is also found to be in nice agreement

with the global best fit value and comfortable with the predictions of the three mixing angles. In conclusion, the charged lepton correction scheme studied can accommodate the current global analysis data with nice precision.

Acknowledgment

The author would like to thank Dr. Subhankar Roy of Gauhati University, Guwahati, for his help in fixing some technical difficulties related to this work.

A Equivalent parametrizations

Here we have shown the equivalence between two parametrizations of mixing matrices that are related to this work. Let us consider the parametrization defined in Eq.(4). Hermitian conjugation of the lepton mixing matrix is

$$U^\dagger = P_2^\dagger V^\dagger P_1^\dagger, \quad (\text{A.1})$$

where

$$P_1^\dagger = \begin{pmatrix} e^{-i\phi_1} & 0 & 0 \\ 0 & e^{-i\phi_2} & 0 \\ 0 & 0 & e^{-i\phi_3} \end{pmatrix}, \quad P_2^\dagger = \begin{pmatrix} e^{-i\alpha} & 0 & 0 \\ 0 & e^{-i\beta} & 0 \\ 0 & 0 & 1 \end{pmatrix}, \quad (\text{A.2})$$

and the mixing matrix V is defined in Eq.(5). Expanding V in terms of three rotation matrices we have

$$U^\dagger = P_2^\dagger R_{12}^\dagger \tilde{U}_{13}^\dagger R_{23}^\dagger P_1^\dagger, \quad (\text{A.3})$$

with

$$R_{12} = \begin{pmatrix} c_{12} & s_{12} & 0 \\ -s_{12} & c_{12} & 0 \\ 0 & 0 & 1 \end{pmatrix}, \quad R_{23} = \begin{pmatrix} 1 & 0 & 0 \\ 0 & c_{23} & s_{23} \\ 0 & -s_{23} & c_{23} \end{pmatrix}, \quad (\text{A.4})$$

$$\tilde{U}_{13} = \begin{pmatrix} c_{13} & 0 & s_{13}e^{-i\delta} \\ 0 & 1 & 0 \\ -s_{13}e^{i\delta} & 0 & c_{13} \end{pmatrix}. \quad (\text{A.5})$$

Now, commuting the phase matrix P_1^\dagger step by step to the right in Eq.(A.1), it can be shown that the parametrization in Eq.(A.1) is equivalent to

$$U^\dagger = P^\dagger U_{12}^\dagger U_{13}^\dagger U_{23}^\dagger, \quad (\text{A.6})$$

where $P^\dagger = P_2^\dagger P_1^\dagger$ and

$$U_{12}^\dagger = \begin{pmatrix} c_{12} & -s_{12}e^{i\delta_{12}} & 0 \\ s_{12}e^{-i\delta_{12}} & c_{12} & 0 \\ 0 & 0 & 1 \end{pmatrix}, \quad U_{13}^\dagger = \begin{pmatrix} c_{13} & 0 & -s_{13}e^{i\delta_{13}} \\ 0 & 1 & 0 \\ s_{13}e^{-i\delta_{13}} & 0 & c_{13} \end{pmatrix}, \quad (\text{A.7})$$

$$U_{23}^\dagger = \begin{pmatrix} 1 & 0 & 0 \\ 0 & c_{23} & -s_{23}e^{i\delta_{23}} \\ 0 & s_{23}e^{-i\delta_{23}} & c_{23} \end{pmatrix}. \quad (\text{A.8})$$

The new phases defined in the matrices U_{12} , U_{13} and U_{23} are related to the phases of the former parametrization as

$$\delta_{12} = \phi_1 - \phi_2, \quad \delta_{13} = \delta - \phi_1 + \phi_3, \quad \delta_{23} = \phi_2 - \phi_3. \quad (\text{A.9})$$

B Higher order expressions for mixing parameters

The expressions for the lepton mixing angles and the Jarlskog invariant given in Eqs.(38), (39), (40) and (42) are approximated up to second order in λ_{ij} where higher order terms are neglected in view of the observation $O(\lambda_{ij}) \sim O(0.1)$. Here we have added higher order terms in these expressions with $O(\lambda_{ij})$ increased by one. Before writing down the expressions we define the following compact notations for convenience :

$$\begin{aligned} \Lambda(12, 13)_{c\pm/s\pm}^{(1)} &= \lambda_{12} \cos \delta_{12}^l \pm \lambda_{13} \cos \delta_{13}^l / \lambda_{12} \sin \delta_{12}^l \pm \lambda_{13} \sin \delta_{13}^l, \\ \Lambda(12, 23)_{c\pm/s\pm}^{(2)} &= \lambda_{12} \lambda_{23} \cos(\delta_{12}^l \pm \delta_{23}^l) / \lambda_{12} \lambda_{23} \sin(\delta_{12}^l \pm \delta_{23}^l), \\ \Lambda(23, 13)_{c\pm/s\pm}^{(2)} &= \lambda_{23} \lambda_{13} \cos(\delta_{23}^l \pm \delta_{13}^l) / \lambda_{23} \lambda_{13} \sin(\delta_{23}^l \pm \delta_{13}^l), \\ \Lambda(12, 13)_{c\pm/s\pm}^{(2)} &= \lambda_{12} \lambda_{13} \cos(\delta_{12}^l \pm \delta_{13}^l) / \lambda_{12} \lambda_{13} \sin(\delta_{12}^l \pm \delta_{13}^l), \\ \Lambda^{(3)} &= (\lambda_{12}^2 - \lambda_{13}^2) \lambda_{23} \cos \delta_{23}^l. \end{aligned} \quad (\text{B.1})$$

With these relevant expressions become

$$\begin{aligned} \sin^2 \theta_{13} &= (s_{13}^\nu)^2 - \sqrt{2} s_{13}^\nu \left[\Lambda(12, 13)_{c+}^{(1)} - \Lambda(12, 23)_{c+}^{(2)} + \Lambda(23, 13)_{c-}^{(2)} \right] \\ &\quad + \frac{1}{2} \left[\lambda_{12}^2 + \lambda_{13}^2 + 2\Lambda(12, 13)_{c-}^{(2)} \right] - \Lambda^{(3)} + \frac{1}{2} (\lambda_{12}^2 + \lambda_{13}^2) \lambda_{23}^2 \\ &\quad - \lambda_{12} \lambda_{23}^2 \lambda_{13} \cos(\delta_{12}^l + 2\delta_{23}^l - \delta_{13}^l), \end{aligned} \quad (\text{B.2})$$

$$\begin{aligned} \sin^2 \theta_{23} &\simeq \frac{1}{2} - \lambda_{23} \cos \delta_{23}^l - \frac{1}{4} \left[\lambda_{12}^2 - \lambda_{13}^2 + 2\Lambda(12, 13)_{c-}^{(2)} \right] \\ &\quad + \frac{1}{\sqrt{2}} s_{13}^\nu \left[\Lambda(12, 13)_{c-}^{(1)} - \Lambda(12, 23)_{c+}^{(2)} - \Lambda(23, 13)_{c-}^{(2)} \right] \\ &\quad + \frac{1}{2} \left[2\sqrt{2} s_{13}^\nu \Lambda(12, 13)_{c+}^{(1)} - (s_{13}^\nu)^2 - \lambda_{12}^2 + \lambda_{23}^2 \right] \lambda_{23} \cos \delta_{23}^l \\ &\quad - \Lambda(12, 13)_{s-}^{(2)} \lambda_{23} \sin \delta_{23}^l, \end{aligned} \quad (\text{B.3})$$

$$\begin{aligned}
\sin^2 \theta_{12} \simeq & \sin^2 \theta'_{12} \left[1 - \lambda_{12}^2 - \lambda_{13}^2 + 2\Lambda(12, 13)_{c-}^{(2)} - 2\Lambda^{(3)} \right] + \frac{1}{2} (\lambda_{12}^2 + \lambda_{13}^2) \\
& - \Lambda(12, 13)_{c-}^{(2)} + \frac{1}{2}\Lambda^{(3)} + \sqrt{2} \sin^2 \theta'_{12} s'_{13} \left[\Lambda(12, 23)_{c+}^{(2)} - \Lambda(23, 13)_{c-}^{(2)} \right] \\
& \mp \frac{1}{\sqrt{2}} \sin 2\theta'_{12} \left[\Lambda(12, 13)_{s-}^{(1)} \left(1 + \Lambda(12, 13)_{c-}^{(2)} \right) + \Lambda(12, 23)_{s+}^{(2)} - \Lambda(23, 13)_{s-}^{(2)} \right] \\
& \pm \frac{1}{2\sqrt{2}} \sin 2\theta'_{12} \left[\sqrt{2} s'_{13} \left(\lambda_{12}^2 \sin 2\delta'_{12} - \lambda_{13}^2 \sin 2\delta'_{13} \right) - (s'_{13})^2 \Lambda(12, 13)_{s-}^{(1)} \right], \quad (\text{B.4})
\end{aligned}$$

$$\begin{aligned}
J \simeq & \pm \frac{1}{2} s'_{12} c'_{12} s'_{13} (c'_{13})^2 \left[1 - 2\lambda_{12}^2 - 2\lambda_{23}^2 - 2\lambda_{13}^2 - \Lambda(12, 13)_{c-}^{(2)} - 2\Lambda(12, 13)_{c+}^{(2)} \right] \\
& \pm \frac{1}{2\sqrt{2}} s'_{12} c'_{12} (s'_{13})^2 c'_{13} \left(3\lambda_{12} \cos \delta'_{12} + \lambda_{13} \cos \delta'_{13} \right) \\
& \mp \frac{1}{2\sqrt{2}} s'_{12} c'_{12} (c'_{13})^3 \left[1 - \frac{3}{2}\lambda_{12}^2 - \lambda_{23}^2 - \frac{1}{2}\lambda_{13}^2 \right] \Lambda(12, 13)_{c+}^{(1)} \\
& \pm \frac{1}{2\sqrt{2}} s'_{12} c'_{12} (c'_{13})^3 \left[\Lambda(12, 23)_{c-}^{(2)} - \Lambda(23, 13)_{c+}^{(2)} - (\lambda_{12}^2 - 2\lambda_{13}^2) \lambda_{12} \cos \delta'_{12} \right] \\
& + \frac{1}{2\sqrt{2}} (s'_{12})^2 s'_{13} (c'_{13})^3 \left[\Lambda(12, 13)_{s-}^{(1)} + \Lambda(12, 23)_{s-}^{(2)} - \Lambda(23, 13)_{s+}^{(2)} \right] \\
& - \frac{1}{2\sqrt{2}} (c'_{12})^2 s'_{13} c'_{13} \left[\Lambda(12, 13)_{s-}^{(1)} - 2\lambda_{12}\lambda_{23} \cos \delta'_{12} \cos \delta'_{23} + \Lambda(23, 13)_{s+}^{(2)} \right] \\
& - \frac{1}{2} \left[(s'_{12})^2 (c'_{13})^2 - (c'_{12})^2 \right] (c'_{13})^2 \Lambda(12, 13)_{s-}^{(2)}. \quad (\text{B.5})
\end{aligned}$$

References

- [1] D. Adey *et al.* (Daya Bay Collab.), *Phys. Rev. Lett.* **121**, 241805 (2018).
- [2] G. Bak *et al.* (RENO Collab.), *Phys. Rev. Lett.* **121**, 201801 (2018).
- [3] H. de Kerret *et al.* (Double Chooz Collab.), arXiv:1901.09445 [hep-ex].
- [4] K. Abe *et al.* (T2K Collab.), *Phys. Rev. Lett.* **121**, 171802 (2018).
- [5] P. Adamson *et al.* (NO ν A Collab.), *Phys. Rev. Lett.* **118**, 231801 (2017).
- [6] M. G. Aartsen *et al.* (IceCube Collab.), *Phys. Rev. Lett.* **120**, 071801 (2018).
- [7] P. F. de Salas *et al.*, *Phys. Lett. B* **782**, 633 (2018).
- [8] I. Esteban *et al.*, *JHEP* **01**,106 (2019).
- [9] P. F. Harrison and W. G. Scott, *Phys. Lett. B* **547**, 219 (2002).
- [10] K. S. Babu, E. Ma and J. W. F. Valle, *Phys. Lett. B* **552**, 207 (2003).
- [11] W. Grimus and L. Lavoura, *Phys. Lett. B* **579**, 113 (2004).

- [12] Z.-Z. Xing and Z.-H. Zhao, *Rep. Prog. Phys.* **79**, 076201 (2016).
- [13] R. N. Mohapatra and C. C. Nishi, *Phys. Rev. D* **86**, 073007 (2012).
- [14] R. N. Mohapatra and C. C. Nishi, *JHEP* **08**, 092 (2015).
- [15] C. C. Nishi, *Phys. Rev. D* **93**, 093009 (2016).
- [16] X.-G. He, *Chin. J. Phys.* **53**, 100101 (2015). arXiv:1504.01560v3 [hep-ph]
- [17] C.-C. Li, J.-N. Lu and G.-J. Ding *Nucl. Phys. B* **913**, 110 (2016).
- [18] E. Ma, A. Natale and O. Popov, *Phys. Lett. B* **746**, 114 (2015).
- [19] Z.-C. Liu, C.-X. Yue and Z-H Zhao *JHEP* **10**,102 (2017).
- [20] S. F. King and Y-L. Zhou *JHEP* **05**, 217 (2019).
- [21] N. Nath, Z.-z. Xing and J. Zhang *Eur. Phys. J. C* **78**, 289 (2018).
- [22] N. Nath *Phys. Rev. D* **99**, 035026 (2019).
- [23] W. Rodejohann and X.-J. Xu *Phys. Rev. D* **96**, 055039 (2017).
- [24] Z.-z. Xing and J.-y. Zhu *Chin. Phys. C* **41**, 123103 (2017).
- [25] C. C. Nishi and B. L. Sanchez-Vega, *JHEP* **01**, 068 (2017).
- [26] Z.-h Zhao *Nucl. Phys. B* **935**, 129 (2018).
- [27] K. Chakraborty, S. Goswami and B. Karmakar *Phys. Rev. D* **100**, 035017 (2019).
- [28] C. Jarlskog *Phys. Rev. Lett.* **55**, 1039 (1985).
- [29] K. A. Hochmuth, S. T. Petcov and W. Rodejohann *Phys. Lett. B* **654**, 117 (2007).
- [30] R. N. Mohapatra and W. Rodejohann *Phys. Rev. D* **72**, 053001 (2005).
- [31] F. Plentinger and W. Rodejohann *Phys. Lett. B* **625**, 264 (2005).
- [32] S. F. King *JHEP* **09**,011 (2002).
- [33] S. Antusch and S. F. King *Phys. Lett. B* **631**, 42 (2005).
- [34] D. Marzocca *et al.*, *JHEP* **11**, 009 (2011).
- [35] D. Marzocca *et al.*, *JHEP* **05**, 073 (2013).
- [36] C. Duarah, A. Das and N. N. Singh *Phys. Lett. B* **718**, 147 (2012).
- [37] S. Roy and N. N. Singh *Indian J. Phys.* **88**, 513 (2014).
- [38] S. Dev, R. R. Gautam and L. Singh *Phys. Rev. D* **89**, 013006 (2014).
- [39] S. Dev, S. Gupta and R. R. Gautam *Phys. Lett. B* **704**, 527 (2011).
- [40] S. Roy and N. N. Singh *Phys. Rev. D* **92**, 036001 (2015).